Metrology camera system of prime focus spectrograph for Subaru telescope

Shiang-Yu Wang, Richard C. Y. Chou, Pin-Jie Huang, Yin-Chang Chang, Hung-Hsu Ling, et al.

Shiang-Yu Wang, Richard C. Y. Chou, Pin-Jie Huang, Yin-Chang Chang, Hung-Hsu Ling, Chi-Hung Yan, Jennifer Karr, Shu-Fu Hsu, Hsin-Yo Chen, Yen-Shan Hu, James E. Gunn, Dan J. Reiley, Naoyuki Tamura, Naruhisa Takato, Yuki Moritani, Atsushi Shimono, "Metrology camera system of prime focus spectrograph for Subaru telescope," Proc. SPIE 10702, Ground-based and Airborne Instrumentation for Astronomy VII, 107027H (9 July 2018); doi: 10.1117/12.2311902

SPIE.

Event: SPIE Astronomical Telescopes + Instrumentation, 2018, Austin, Texas, United States

Metrology Camera System of Prime Focus Spectrograph for Subaru Telescope

Shiang-Yu Wang*[a], Richard C. Y. Chou[a], Pin-Jie Huang[a], Yin-Chang Chang[a], Hung-Hsu Ling[a], Chi-Hung Yan[a] , Jennifer Karr[a], Shu-Fu Hsu[a], Hsin-Yo Chen[a], Yen-Shan Hu[a], James E. Gunn[b], Dan J. Reiley[c], Naoyuki Tamura[d], Naruhisa Takato[e], Yuki Moritani[d], Atsushi Shimono[d]
[a]Academia Sinica, Institute of Astronomy and Astrophysics, P. O. Box 23-141, Taipei, Taiwan;
[b]Princeton University, Princeton, New Jersey, 08544, USA;
[c]California Institute of Technology, 1200 E California Blvd, Pasadena, CA 91125, USA;
[d]Kavli Institute for the Physics and Mathematics of the Universe (WPI),The University of Tokyo Institutes for Advanced Study, The University of Tokyo, Kashiwa, Chiba 277-8583, Japan;
[e]Subaru Telescope, National Astronomical Observatory of Japan, 650 North A'ohoku Place Hilo, HI 96720, U.S.A.

ABSTRACT

The Prime Focus Spectrograph (PFS) is a new optical/near-infrared multi-fiber spectrograph designed for the prime focus of the 8.2m Subaru telescope. PFS will cover a 1.3 degree diameter field with 2394 fibers to complement the imaging capabilities of Hyper SuprimeCam. To retain high throughput, the final positioning accuracy between the fibers and observing targets of PFS is required to be less than 10 μm. The metrology camera system (MCS) serves as the optical encoder of the fiber positioners for the configuring of fibers. MCS provides the fiber positions within a 5 microns error over the 45 cm focal plane. The information from MCS will be fed into the fiber positioner control system for the closed loop control.
MCS locates at the Cassegrain focus of Subaru telescope to cover the whole focal plan with one 50M pixel Canon CMOS camera. It is a 380 mm aperture Schmidt type telescope which generates uniform spot size around 10 μm FWHM across the field for reasonable sampling of the point spreading function. An achromatic lens set is designed to remove the possible chromatic error due to the variation of the LED wavelength. Carbon fiber tubes are used to provide stable structure over the operation conditions without focus adjustments. The CMOS sensor can be read in 0.8 s to reduce the overhead for the fiber configuration. The positions of all fibers can be obtained within 0.5 s after the readout of the frame. This enables the overall fiber configuration to be less than 2 minutes. MCS is installed inside a standard Subaru Cassgrain Box. All components generate heat are located inside a glycol cooled cabinet to reduce the possible image motion due to the heat. The integration of MCS started from fall 2017 and it was delivered to Subaru in April 2018.
In this report, the performance of MCS after the integration and verification process in ASIAA and the performance after the delivery to Subaru telescope are presented.

Keywords: Metrology, CMOS sensor, multi-fiber, spectrograph, Schmidt telescope

1. INTRODUCTION

The Prime Focus Spectrograph (PFS) is a new prime focus optical/near-infrared multi-fiber spectrograph for the 8.2 m Subaru telescope[1]. PFS will cover a 1.3 degree diameter field with 2394 fibers to complement the imaging capabilities of Hyper SuprimeCam[2]. To retain high throughput, the final positioning accuracy between the fibers and observing targets of PFS is required to be less than 10 μm. The metrology camera serves as the optical encoder of the fiber motors for the configuring of fibers[3]. The metrology camera system (MCS) is designed to provide the fiber position information within 5 μm error over the 45 cm focal plane. The information from the metrology camera will be fed into the fiber positioner control system for the closed loop control.

The MCS will be located at the Cassegrain focus of Subaru telescope to cover the whole prime focal plane with one 50 M pixel Canon CMOS sensor. To reduce high spatial frequency distortion of the wide field corrector (WFC), the

* sywang@asiaa.sinica.edu.tw; phone 886 2 2366-5338; fax 886 2 2367-7849; www.asiaa.sinica.edu.tw

Ground-based and Airborne Instrumentation for Astronomy VII, edited by Christopher J. Evans, Luc Simard, Hideki Takami, Proc. of SPIE Vol. 10702, 107027H · © 2018 SPIE · CCC code: 0277-786X/18/$18 · doi: 10.1117/12.2311902

aperture size of the metrology camera is set to be 380 mm which is the largest affordable aperture at the Suabru Cassegrain focus[4]. A Schmidt telescope type optical design was adapted to provide uniform image quality across the field with reasonable sampling of the point spread function (PSF). An achromatic lens set was designed to prevent the possible chromatic shift of the images due to the change of backlight LEDs. The mechanical design based on Invar and carbon fiber tubes provides stable structure over the temperature range under operating conditions. The CMOS sensor can be read in 0.8 s to reduce the overhead for the fiber configuration[4]. The positions of all fibers can be obtained within 0.5 s after the exposure is finished. This enables the overall fiber configuration to be less than 2 minutes.

The PFS collaboration is led by the Kavli Institute for the Physics and Mathematics of the Universe of the University of Tokyo with international partners consisting of Academia Sinica, Institute of Astronomy and Astrophysics in Taiwan, Caltech/Jet Propulsion Laboratory, Princeton University, Johns Hopkins University in USA, the Chinese PFS Participating Consortium in China, the Laboratoire d'Astrophysique de Marseille in France, the Max Planck Institute for Astrophysics and Max Planck Institute for Extraterrestrial Physics in Germany, the National Astronomical Observatory of Japan/Subaru Telescope, the Brazilian consortium where Universidade de de São Paulo/Laboratório Nacional de Astrofísica are the main contriubutors, and the NorthEast Partitipation Group in USA that has very recently joined.

2. METROLOGY CAMERA FUNCTIONS AND COMPONENTS

The MCS will be installed inside a Cassegrain instrument box like other Subaru Cassegrain instruments. Figure 1 shows the 3D model of the MCS inside the instrument box. Calibration of the image distortion and mapping to the focal plane through the WFC is achieved by back-lit fixed fiducial fibers and home positions of scientific fibers. The home positions of the science fibers have been tested to provide good repeatability (~1 μm) after rotational movements. The positions for the fiducial fibers and home positions of science fibers will be measured to a high repeatable accuracy during the integration and verification of the fiber system.

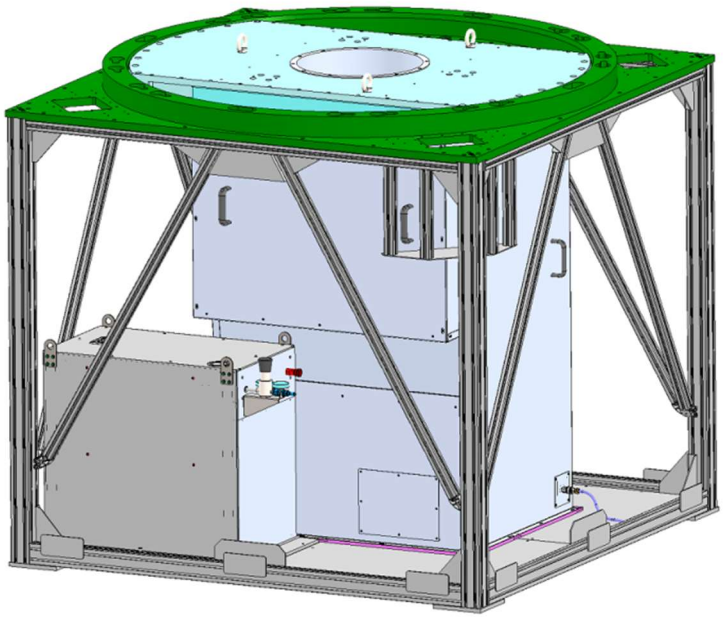

Figure 1. The 3D model of MCS inside the standard Subaru Cassegrain instrument box

In the beginning of each COBRA fiber positioner configuration, the positioners will move to the home positions to generate reference points across the field for distortion map confirmation. After that, the science fibers will move to new positions based on the chosen target to fiber assignment. The MCS will measure the location of each fiber position with the sensor coordinate system and send it to the PFI control system. Then, fiber position errors are calculated with respect to the required locations for the fibers. This iteration will be repeated a number of times until the errors converge to the expected value. The back illuminator of fiducial and science fibers will be turned on throughout the iterations. In addition, MCS also supports two additional diagnostic functions during the commissioning and engineering phases. The first is to image the circular motion of the fibers to obtain the rotational center of the motors. During such an operation, a

series of images will be taken with fibers stopping at several positions on the circular moving trajectories. MCS will calculate the center positions of the trajectories with high precision. The second function is to generate fiber images when the prime focus instrument rotator is moving while COBRA positioners stay still. With several exposures during the rotator movement, the metrology camera will capture the arcs generated by the fibers and estimate the offset and tilt between the rotator axis and the fibers focal plane center.

2.1. MCS hardware

The metrology camera has fast optics (f/2.2) to accommodate the 380 mm aperture size and a focal length of 847 mm. The Schmidt reflector design allows a compact system to fit into the Subaru Cassegrain box with a height limit of 1750 mm. The camera optics consists of an achromatic corrector, a Schmidt plate, a spherical mirror, a field flattener and a color filter. In order to generate well sampled image spots, the Schmidt plate was deliberately designed to under correct the spherical aberration. The predicted spot size of the fiber tip extends about 9 μm or ~3 pixels. The shape of the PSFs over the entire field is quite uniform and satisfies the centroid estimation requirement. The image distortion at the field edge is 0.1% which is much smaller than the distortion of wide field corrector (WFC) (2.5%).

Two different illuminator sources are used to illuminate the science and fiducial fibers. Although the same type of LEDs are used for both illuminators, small shifts of the wavelength might still happen due to different LED batches, different operation temperatures and power. Our simulation showed that a 1 nm wavelength change of the LED emission central wavelength generates a chief ray shift of about 0.05 μm and a PSF centroid shift of 0.1 μm on the MCS image plane. This corresponds to a 2.6 μm shift on the PFI focal plane. The error is not acceptable if we have the LED shift more than 2nm. To prevent the possible chromatic shift of the PSF due to the wavelength change of back illumination LEDs, an achromatic lens set was added to reduce the chromatic error of the telescope. The achromatic lens should be designed to correct the chromatic error of 5-10 nm LED wavelength change.

The concept of the achromatic corrector is to use a doublet lens system to correct the optical path difference of different wavelengths. This means the doublet lens system should cover the whole aperture of the MCS. Ideally, the lens system can be designed to be powerless so that it can be added on the original metrology camera without any change of the position of the optics or focal plane. However, such design requires a surface figure with a large radius of curvature which is not easy to achieve. In practice, we changed the first surface of the achromatic to be a flat surface. The drawback of this design is that the achromatic lens set requires the change of the focal position of the MCS by +5.78 mm. The MCS camera module has to be shimmed to lift by 5.78 mm. The X and Y position of the PSF at different locations of the MCS FoV with different LED peak wavelength are plotted in figure 2. The chromatic deviation of the spot locations with a 5 nm wavelength shift is smaller than 0.04 μm which is less than 1 μm at the focal plane.

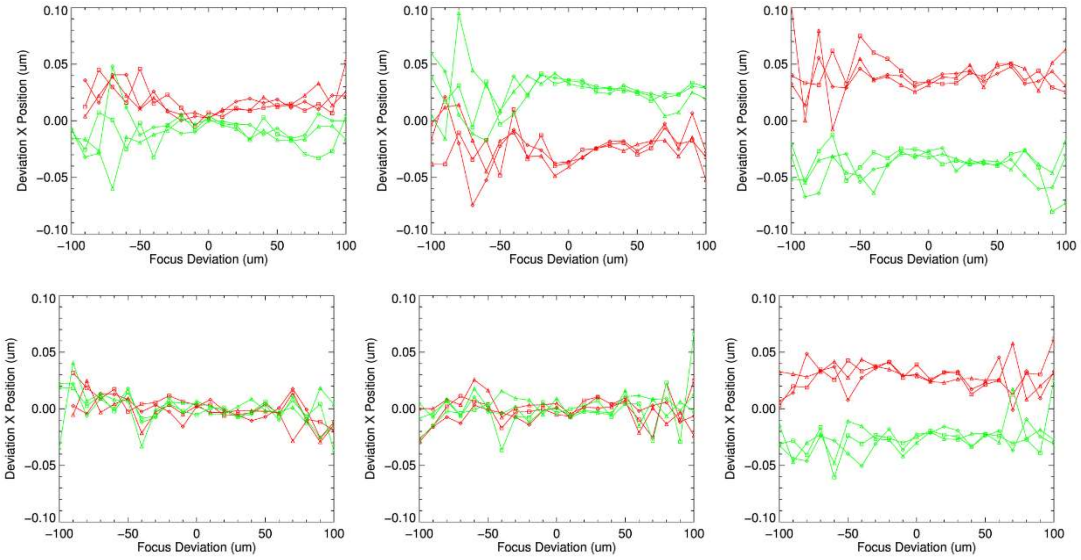

Figure 2. PSF chromatic deviations with the achromatic lens system. Different symbols indicate different sub pixel shifts of the chief ray respected to the pixel center. Red curves represent an LED peak shift of + 5nm; green curves represent an LED peak shift of -5 nm. The fluctuation of PSF deviations get stronger when the defocus is greater than -50 μm, but

most cases still fall within +/-0.04 μm. From left to right are plots with the object at (0, 0), (0, 238.5) and (168, -168) mm at the Subaru prime focal plane.

The camera sensor used is a 50 M pixel CMOS sensor with 8960 × 5778 pixels and 3.2 μm pixel size developed by Canon Inc.. The effective pixel number is 8832 × 5748 pixels. This large format sensor can cover the entire focal plane and provide the required centroid estimation accuracy of fibers with a single exposure. The physical size of the sensor is about 28.67 mm × 18.49 mm. It is a front-side illuminated sensor with a micro-lens on every pixel to improve the light collection efficiency. With the current optical design, each fiber image will be sampled by roughly 3 pixels for the 10μm FWHM spots. The camera only supports continuous video mode operation with the rolling shutter. A mechanical shutter is used to control the exposure time and duration. Once the exposure starts, the frame grabber card will save the frames from the camera until the exposure ends and save the final frame after the shutter is closed to ensure all signal is collected when the shutter is open. All frames will be co-added to produce the final MCS image for centroid calculation.

The design principle for the MCS mechanical structure is to reduce possible adjustments during observations. The main supporting structure is made of carbon fiber tubes to ensure very low thermal expansion and low deformation due to gravity. As a Subaru Cassegrain instrument, the mechanical structure for the metrology camera should meet the space and mounting scheme as for other Cass instruments. The weight of the main metrology camera structure is about 322 kg, including the mechanical structures and optics but without the interface plate. The mechanical structure for the metrology camera can be separated into two components: 1) the main system with supporting and mounting structure for the optical elements and camera sensor module; 2) the electronic box with all electronic devices and the host computer. The interface plate is connected to the Cassegrain box which can provide high repeatability to the telescope structure. It also carries the counter weight needed for the whole Cassegrian box. MCS reuses the old Subaru Kyoto 3D instrument Cassegrain box. It has been used to show the installation repeatability around 200 μm. The total weight of MCS and the Cassegrain box is around 2285 kg. The components which generate heat are located inside the sealed electronic box with glycol cooling to keep the surrounding ambient temperature of the Cassegrain box stable. The MCS main body is also covered with dry air purge to prevent the possible condensation during the high humidity conditions.

The details of the MCS components could be found in the previous SPIE proceedings[4,5].

2.2 MCS software

The main task of the MCS control system is to identify the science and fiducial fibers and measure the centroids of fiber spots, including image acquisition. Figure 3 shows the control system architecture. The measured centroids, along with fiber identifications, are then sent to motor control software, while the image is saved locally.

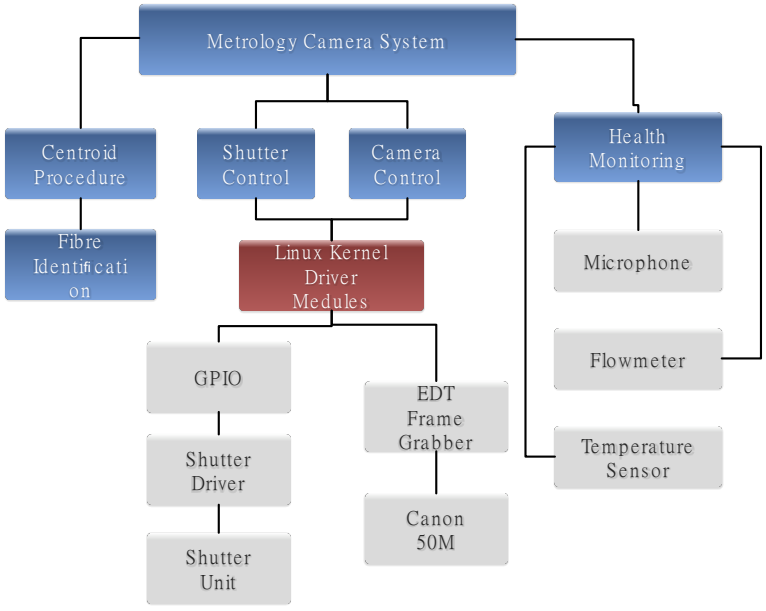

Figure 3 : The control system architecture of MCS.

To achieve this operation, MCS controls the camera and shutter through the Linux driver modules. The control system sends a GPIO signal to the shutter driver and commands the shutter to move. Meanwhile, the camera image is ready for readout with EDT frame grabber. The low-level control of the shutter and camera is performed with C programs. These C APIs are then wrapped with Python and integrated into messaging hub system (MHS). There are only two modes for image acquisition with shutter open or closed. The images will be reduced as needed for analysis (pixel sensitivity adjustments, pixel DC offsets, and the exclusion of bad pixels), however the raw uncalibrated images will be saved for later analysis if needed. Calibration images (bias, dark, flats) will be taken as part of engineering process, as they require a special setup, rather than during observations; the names of the calibration files will be stored locally in the MCS configuration files.

For a given observation ID, the MCS system can access relevant parameters (flat-field and other calibration data, target positions, COBRA centres, MCS configuration file) from the database, and will write to the database as needed. This process primarily occurs within the MCS system. The details of the control software and the operation manual will be provided in a separated document. The centroid calculation algorithm is very important to provide solid centroid calculation in a short time for all fibers. Based on our tests with FMOS fiber images and simulated PFS data, we have developed a modified DAOPHOT algorithm for the spot detection, combined with centroid fitting using the mpfit library, which uses an implementation of the Levenberg-Marquardt technique.

The algorithm first performs a threshold to identify pixels above a given noise level, then performs a convolution of these pixels with a Gaussian kernel to smooth out pixel to pixel noise. Most of the image is noise, so this initial thresholding increases computational speed. In addition, the convolution has been separated into two 1D convolutions, and performed using integer arithmetic, both of which speed up the process.

A basic peak finding routine is then run on the smoothed pixels, identifying local maxima as candidate points. The candidate points are then filtered using criteria of central concentration and shape, which reject cosmic rays, hot pixels and other artifacts. A fit is then calculated for each spot, calculating the centroids, as well as the FWHMs, peak value, and background. Three possible fitting algorithms were developed; the fast algorithm with a simple weighted centre of mass but less accurate (and does not provide shape information), the slow algorithm with a 2D Gaussian fit which is the most robust, and the intermediate algorithm that fits 1D Gaussians along each axis and interpolates the centroid. The MCS uses the fast algorithm for the first few iteration of target convergence while the intermediate algorithm will be used for the rest of iterations which requires higher accuracy. The slow algorithm is a backup in case the intermediate algorithm is not accurate enough.

In addition, the code has been parallelized using threads, for increased speed. The image is divided into overlapping subimages, which are analyzed in parallel, and the results combined. The threads do not share resources, which makes the parallelization relatively simple. The computational expense is dominated by the time for the centroid fits and the Gaussian smoothing. The code itself is written in C and is called from python via a Cython wrapper.

3. METROLOGY CAMERA PERFORMANCE

As mentioned, the MCS is designed to provide fiber position information within 5 μm error over the 45 cm focal plane of PFS. The optical system is the key to provide reasonable image quality so that the fiber spots can be well measured in order to achieve the 5 μm error. The assembly, integration and test processes of MCS were detailed in the reference[5]. The MCS is positioned ~18 meter from a 14 inch pin hole mask which is used to mimic the science fibers. The pin holes on the mask have the same diameter as the science fibers (127 μm) so as to generate similar image spots on the MCS camera. On the pin hole mask, there are two sets of holes; one with separations of 8 mm and the other one with separations of 2mm. 8mm is the nominal distance between the two Cobras and 2 mm is the closest possible distance between two science fibers. The total spots number on the mask is about 3500 which is much more than the number of fibers in PFS (~2500).

Between the MCS optics and the pin hole mask, there is a folding mirror so that we do not have the find a 18 m vertical space for the alignment work. In the original design, we planned to use a 60 cm mirror to cover the whole MCS aperture. Unfortunately, the mirror prepared was not thick enough and it generated bad aberrations in the image when it was positioned at 45 degrees to the direction of gravity. We had to use a 30 cm diameter mirror instead. Since the mirror aperture is smaller than the MCS aperture, the effective area is smaller along the direction of MCS optical axis with the 45 degree reflection so the image spot is more elongated in the horizontal axis. The pictures of the testing system are

shown in figure 4. The justification criteria for claiming a successful alignment are to achieve uniform PSF size across the entire field with a FWHM equal to 10 μm.

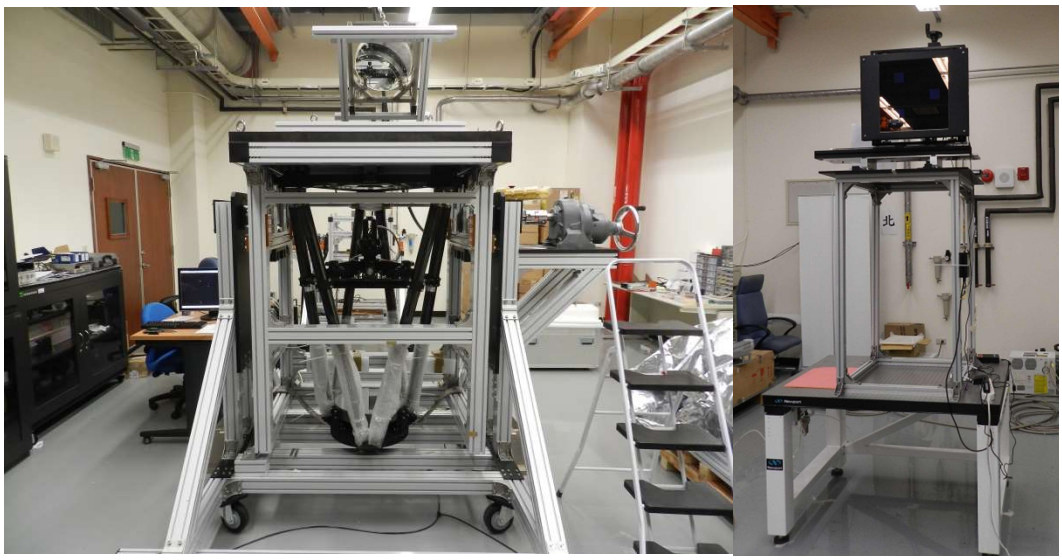

Figure 4. The MCS on the testing stand with the folding mirror (left). The pin hole mask structure used for the alignment (right). The two are separated around 80 m.

3.1. The image quality

This section presents the image quality of the MCS upon delivery. Figure 5 shows the pinhole mask image taken by MCS at a vertical position after we completed the optical alignment. A zoomed in image of a pinhole is presented in the right panel of figure 5. PSFs taken from the top and the right corners of the pinhole mask are also shown in the same panel. The FWHM of the PSF is 2 pixels in the horizontal direction and 3 pixels in the vertical direction. The ZEMAX simulation image shows the FWHM is 2.9 pixels in horizontal direction and 2.1 pixels in vertical direction, consistent with the measured image FWHM. As explained, this is due to the different effective aperture in the horizontal and vertical directions. The image quality is uniform across the entire pinhole mask.

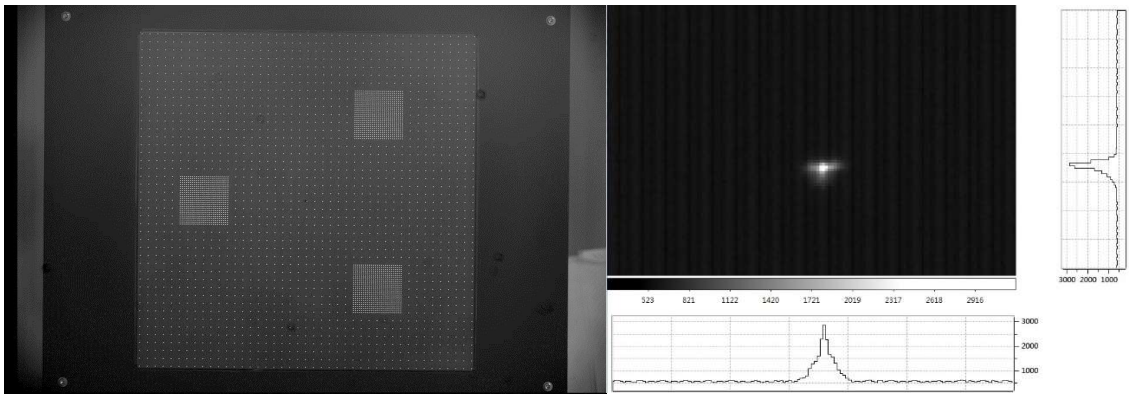

Figure 5. The pin hole mask image taken by MCS after the alignment was completed (left). The close view of the MCS image spot and the psf profiles (right)

In order to confirm the image quality for the full MCS aperture, we tilted the whole MCS to the horizontal position so that the optics could image the pin-hole mask directly without the folding mirror. The left panel of Figure 6 shows the pinhole mask image taken by MCS at the horizontal position. The bright region of the image is due to the stray light in the lab. A zoomed in PSF is presented in eight panel of Figure 6. The FWHM of the PSF is ~ 2.5 pixels in both horizontal and vertical directions. The image quality is quite uniform across the pinhole mask. The full coverage of the MCS aperture reduces the image spot size. The shape of the PSF is slightly different from the PSF taken at the MCS

vertical position. The reason could be the optics gravitational deformation at different elevation angle. The size of the PSF is smaller than the case of vertical test configuration. This gives us a high confidence that the image quality is maintained at different elevation angle of the telescope.

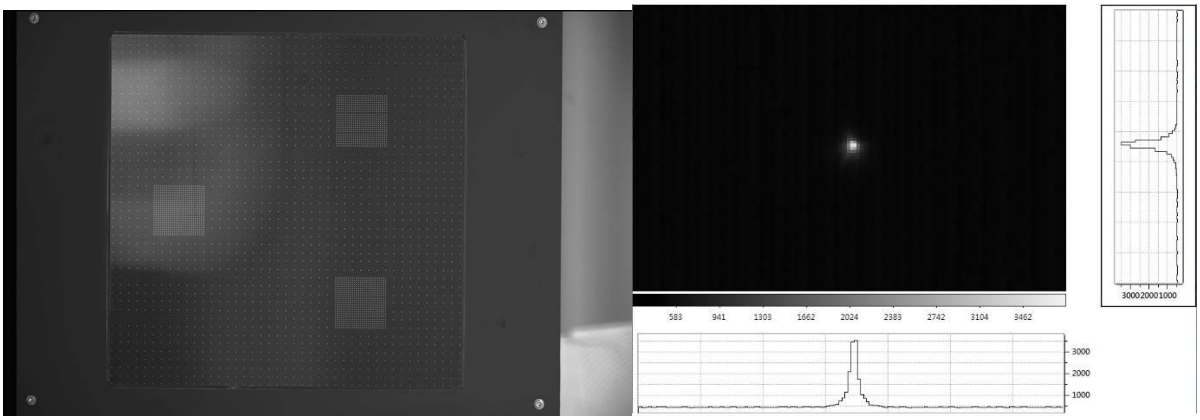

Figure 6. The pin hole mask image taken by MCS with the whole system tilted to the horizontal direction (left). The close view of the MCS image spot and the psf profiles (right)

3.2. Field of View

The FoV of MCS is different with and without the WFC. With the WFC present in the optical system, the MCS FoV can cover the Subaru primary focal plane with a diameter of 489 mm, yielding a magnification rate of 0.037. In the case of the laboratory test stage (i.e., no WFC), the diameter of the object plane covered is only 394 mm instead, yielding a magnification factor of 0.047.

Since we do not have the WFC, we could only check the FoV of MCS without WFC in the lab. We measured the image size taken by MCS without WFC. The actual size for the glass mask is 340 mm, which corresponds to 5004 pixels on the image. This yields a magnification rate of 5004*0.0032/340 = 0.047, which fits the ZEMAX simulation well. Another check for the magnification rate is the pitch of pinholes. The pitch between two pinholes is 8 mm, which corresponds to 118 pixels. The magnification rate can also be calculated by 118*0.0032/8 = 0.047. We are confident that the final FoV should also be close to 489 mm if the data provided for WFC are correct.

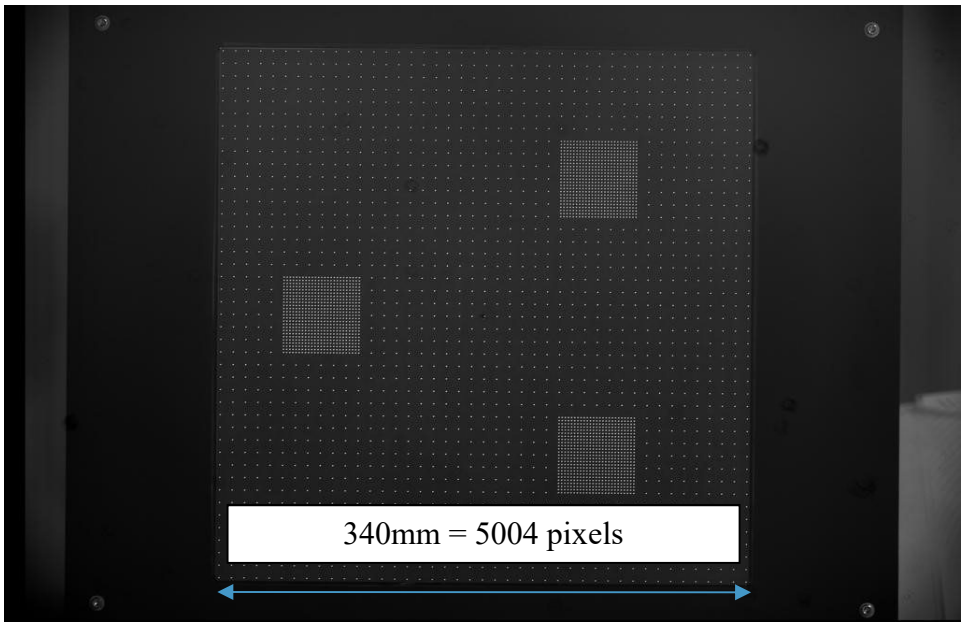

Figure 7. The image size of the pin hole mask image taken by MCS.

3.3 Centroiding accuracy and time

After the optical alignment is completed, the centroid algorithm was tested. In order to minimize the possible turbulence which can increase the image motion for the setup, the air conditioning was turned off during the test. Only one person operating the software was in the lab during the test. 30 images with different exposure times (0.5, 1, 2, 3, 4, 5, and 10 s) were taken to test the centroiding accuracy and speed. The different exposure times were to understand the error from the turbulence in the lab and hopefully to extract the real centroiding algorithm error. In addition, timing tests were performed with the same dataset, in order to understand the time needed for each step of the MCS operation.

For the centroiding accuracy estimation, each image was passed through the centroiding algorithm and the results (x and y position, FWHM in the x and y directions, peak value, and fitted background value) were saved to disk. The spots were then positionally matched between frames. The average position for each spot was then calculated. In addition, the average x position and y position for each exposure were calculated, to determine the global shift in position of the image. This average position was then subtracted from each frame. The RMS variation in the position of the centroid was then calculated for each individual spot. The average FWHM, peak and background were also calculated for each spot.

For diagnostic purposes, we produced several plots to check the quality of the test data. First, a spatial map of the spots, color coded by RMS, was plotted to check the variation of RMS across the field, which was fairly uniform. The average size of the spots (FWHM(x)*FWHM(y) were plotted the same way to check for variations in shape over the field, which was also fairly uniform. The average FWHMs and peak values were plotted as a function of exposure number, to check for time variation; in particular, the average peak value of the spots varied between images, an artifact of the illumination of the pin-hole mask.

Finally, the average RMS variation of the position as a function of exposure time was plotted. Figure 8 shows the RMS as a function of exposure time for both the fast and intermediate algorithms. This confirms the results of initial dome seeing tests conducted at Subaru[4], where it was found that an exposure time shorter than 0.5 s was dominated by seeing effects. The RMS values drop significantly at 1 sec as the seeing effects are smoothed out. The clear difference between the centroid accuracy histogram of 0.5 and 1 sec data with the intermediate algorithm is shown in the upper panel of figure 8. Note that the data at 3 s has been deleted due to an obvious disturbance of the system during the test, which was spotted using the diagnostic images. The centroid accuracy for the fast algorithm is about 0.13 pixels while the slow algorithm can give an accuracy around 0.015 pixels. The test result is consistent with the result done by the simulated images. The distribution is uniform across the FoV. The histogram of the RMS number across the pin-hole mask for 1 s result was also plotted in figure 9.

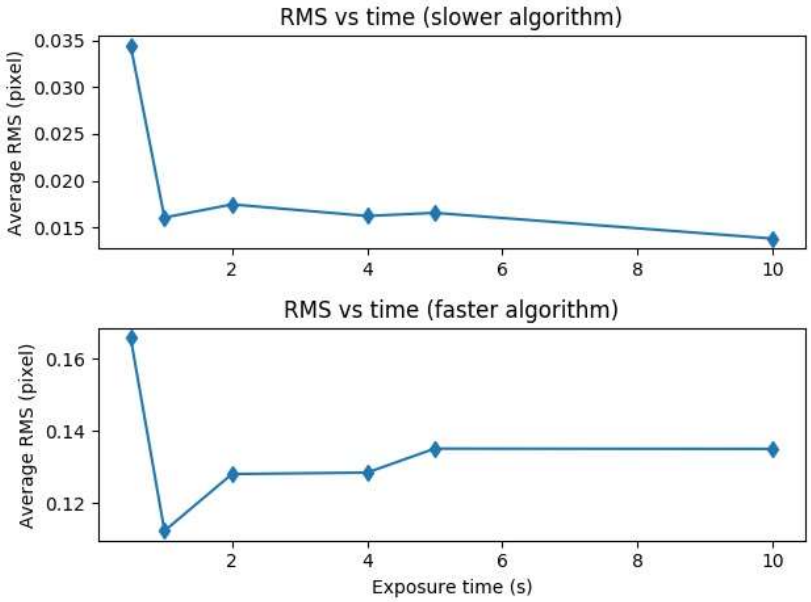

Figure 8. RMS centroid location as a function of exposure time for the intermediate (upper) and fast algorithms (lower).

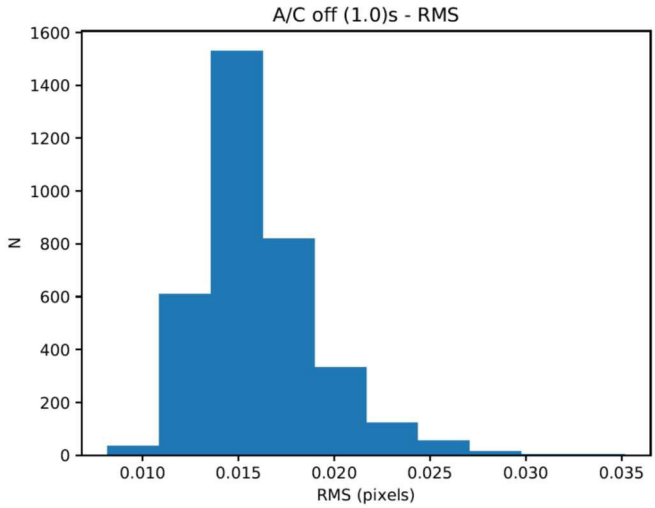

Figure 9. The histogram of RMS centroid location for 1 s exposure.

To test the centroiding speed, we ran the centroiding algorithm only, within MHS, on the MCS computer, using real 1 s exposure data from the pinhole mask, for a loop of 20 iterations, and measured the average processing time. We repeated the test for several configurations of number of cores and centroiding algorithms. The results were in general agreement with previous estimates. For a single core, with the intermediate fitting algorithm, the centroiding time was 0.92 s. With four cores, the time was 0.56 s, and using all 16 cores the time was 0.35 s. This confirmed the expected behavior as a function of the number of cores. With the slowest algorithm (the back up one), the fitting time for all cores was 0.45 s, still within the project requirements. For the fast but lower accuracy algorithm, the time was 0.23 s.

Note that the above numbers do not include the fibre identification step, (which is not needed for the initial MCS testing), but this step is significantly less computationally intensive than the centroiding. However, this number includes all the spots in the pinhole mask, which is about ~30% more than the number of spots in PFS. For 1 sec exposures, three frames are required due to the rolling shutter. All three frames are saved, as well as the co-added image. This takes 3.36 s to complete. For the database insertion, the time to insert 2394 sets of fibre positions and measured parameters was measured 100 times, and averaged, for a result of 0.2 s per exposure. Therefore the total time for a single loop, with the intermediate fitting algorithm and 1 s exposure is 3.91 s. This is well within the 5 s requirement.

4. COMMISSIONING AT SUBARU

The MCS was delivered to Subaru on April 20. Right after the delivery, the functions and the optical alignment was checked at the Subaru telescope Hilo headquarter. However, due to the limitation of the lab space, there is no suitable baseline for the pin hole mask assembly of the image quality check. Instead, we used a laser to confirm the optics center were aligned and leave the real image quality check until MCS is at the summit of Mauna Kea. All other functions were confirmed to be the same as in Taiwan and working properly. Furthermore, the control system was integrated with the Subaru telescope control system and network during the MCS stay in Hilo.

Soon after the performance check in Hilo, the MCS was transported to the summit site of Subaru telescope. The pin hole mask system was set up at the observation floor of the telescope dome to verify the optical quality. The first images showed that the optical alignment was changed during the shipping process. With delicate adjustment, we were able to obtain slightly better image quality. Figure 10 shows the spot size FWHM obtained in Taiwan and in Hawaii.

The MCS was removed from the test frame structure and installed into the Subaru Cassegrain instrument box after the optical alignment. Figure 11 shows the picture taken during the integration and after the integration. The system is now ready for the upcoming engineering runs in June and July 2018. The goals of the engineering run include the system alignment with the telescope, the distortion map generation, the dome seeing test and control software integration and tests.

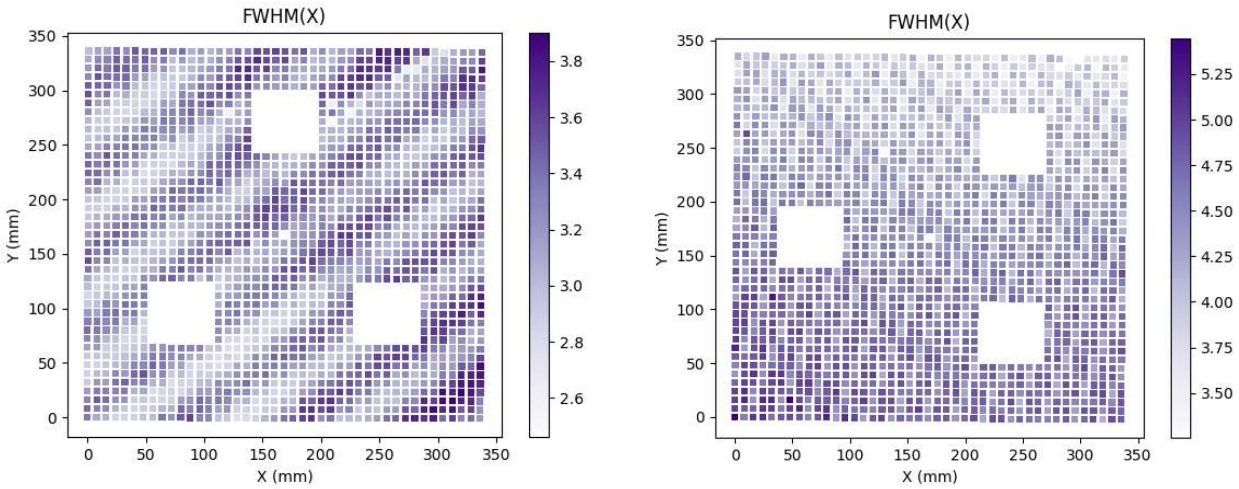

Figure 10. The spot FWHM in X direction for the pin hole mask image taken in Taiwan (left) and in Hawaii (right).

Figure 11. The removal of MCS from the test frame (left). The MCS installed into the Subaru Cassegrain instrument box (right).

5. SUMMARY

The PFS MCS has been integrated and tested. The functions of MCS in the lab have passed the required performance after the integration. The MCS is now integrated into the Subaru instrument box and it is ready for the coming commissioning runs in June and July 2018. The real performance on the telescope will be examined in July 2018.

ACKNOWLEDGEMENT

We gratefully acknowledge support from the Funding Program for World-Leading Innovative R&D on Science and Technology(FIRST) "Subaru Measurements of Images and Redshifts (SuMIRe)", CSTP, Japan for PFS project. The work in ASIAA, Taiwan is supported by the Academia Sinica of Taiwan.

REFERENCES

[1] Komiyama, Y., Aihara, H., Fujimori, H., Furusawa, H., Kamata, Y., Karoji, H., Kawanomoto, S., Mineo, S., Miyatake, H., Miyazaki, S., Morokuma, T., Nakaya, H., Nariai, K., Obuchi, Y., Okura, Y.,

Tanaka, Y., Uchida, T., Uraguchi, F., Utsumi, Y., Endo, M., Ezaki, Y., Matsuda, T., Miwa, Y., Yokota, H., Wang, S.-Y., Liaw, E. J., Chen, H.-Y., Chiu, C.-F., and Jeng, D.-Z., "Hyper Suprime-Cam: Camera Design," Proc. SPIE 7735, 77353F-1 (2010).

[2] Sugai, H. et al. "Prime focus spectrograph: Subaru's future," Proc. SPIE 8446, 84460Y (2012).

[3] Wang, S.-Y., Hu, Y.-S., Yan, C.-H., Chang, Y.-C. Tamura, N., Takato, N., Shimono, A., Karr, J., Ohyama, Y., Chen, H.-Y., Ling. H.-H., Karoji, H., Sugai, H., Ueda, A., "The metrology cameras for Subaru PFS and FMOS," Proc. SPIE 8446, 84464Z (2012).

[4] Wang, S.-Y., Chou, C.-Y., Chang, Y.-C., Huang, P.-J., Hu, Y.-S., Chen, H.-Y., Tamura, N., Takato, N., Ling, H.-H., Gunn, J. E., Karr, J., Yan, C.-H., Mao, P., Ohyama, Y., Karoji, H., Sugai, H., Shimono, A., "Metrology camera system of prime focus spectrograph for Subaru telescope," Proc. SPIE 9147, 91475S (2014).

[5] Wang, S.-Y., Chou, C.-Y., Huang, P.-J., Ling, H.-H., Karr, J., Chang, Y.-C., Hu, Y.-S., Hsu, S.-F., Chen, H.-Y., Gunn, J. E., Railey, D. J., Tamura, N., Takato, N., Shimono, A., " Metrology Camera System of Prime Focus Spectrograph for Subaru Telescope," Proc. SPIE SPIE 9908, 990881 (2016).